Ecotoxicology and Environmental Safety 196 (2020) 110532

Contents lists available at ScienceDirect

Ecotoxicology and Environmental Safety

journal homepage: www.elsevier.com/locate/ecoenv

Unravelling the ZnO-NPs mechanistic pathway: Cellular changes and altered morphology in the gastrointestinal tract of the earthworm *Eisenia andrei*

Zuzanna M. Świątek[a,*], Olga Woźnicka[b], Agnieszka J. Bednarska[c]

[a] Institute of Environmental Sciences, Jagiellonian University, Gronostajowa 7, 30-387, Kraków, Poland
[b] Institute of Zoology and Biomedical Research, Jagiellonian University, Gronostajowa 7, 30-387, Kraków, Poland
[c] Institute of Nature Conservation, Polish Academy of Sciences, Mickiewicza 33, 31-120, Kraków, Poland

ARTICLE INFO

Keywords:
Zinc
Nanoparticles
Chloragogen tissue
Gut epithelium
Morphology

ABSTRACT

A major uptake route of nanoparticles (NPs) occurs via the gastrointestinal (GI) tract. When GI tract cells are exposed, NPs cytotoxic effects are observed that subsequently adversely affect the GI tract morphology and have consequences for the whole organism. The aim of this study was to understand the mechanism of effects caused by ZnO-NPs compared to Zn ions on the earthworm *Eisenia andrei*.

The following aspects of individually exposed earthworms were investigated: 1) qualitative structural alterations in the gut epithelium and chloragogen cells of the GI tract, 2) quantitative changes within chloragogen tissues after 48 h of exposure (using morphometric analysis), and 3) the ADP/ATP ratio in homogenized tissue of the whole organism after 21 days of exposure to contaminated soil (contamination phase) followed by 14 days of elimination in clean soil (decontamination phase) to identify possible recovery.

Both ZnO-NPs and Zn ions adversely affect the gut epithelium and chloragogen tissue of earthworms after 48 h of exposure to contaminated soil. Morphometric measurements revealed that the proportions of debris vesicles in the chloragocytes were significantly lower in worms exposed to ZnO-NPs than in worms exposed to Zn ions. Moreover, numerous spherite granules were observed in the chloragocytes of ionic Zn-treated worms, but not the ZnO-NPs-treated worms, suggesting differential regulation of these Zn forms. The Zn cytotoxic effect was not reflected in ADP/ATP ratio measurements. Our study provides new insights into nano-specific effects that are distinctive from ion regulation inside the GI tract and furthers our understanding of the relationship between effects at the cellular and whole-body levels.

1. Introduction

ZnO nanoparticles (ZnO-NPs) are one of the most frequently produced engineered nanomaterials and have more than 60 applications worldwide, including uses in electronics, chemical products, technical products, cosmetics, and pharmaceuticals (DaNa database). Increasing production and usage of ZnO-NPs are inseparably associated with their release into the different environmental compartments and may lead to hazards to the soil ecosystem (Adam and Nowack, 2017; Loureiro et al., 2018), and hence earthworms and other soil-dwelling organisms (Kwak and An, 2015; Rajput et al., 2018).

Though there is much research on ZnO-NP toxicity performed with *in vitro* studies on different cell cultures (Buerki-Thurnherr et al., 2013; Yu et al., 2013), such results are difficult to extrapolate to the level of whole organisms, so-called *in vivo* systems (Hong et al., 2013). The combination of tools and endpoints covering effects at different levels of biological organization (e.g., cellular, organismal) were indicated to be more desirable and the key for systems (eco)toxicology approach (Amorim et al., 2015). Therefore, linking the cytotoxic effects observed at the cell level with the effects observed in the whole organism may provide additional information of the cytotoxic effects of ZnO-NPs, leading to an improvement in nanoparticle (NP) hazard assessment. Cytotoxicity plays an important role in NP studies (Ajdary et al., 2018; Fröhlich and Fröhlich, 2016). Once in the cellular milieu, NP toxicity can lead to a number of pathological processes, as NPs do not exhibit a specific mechanism of action. Hence, differences in toxicity between ZnO-NPs and Zn ions may be more apparent at the cellular level at the immediate site of their action.

One of the main routes through which NPs can enter organisms is the gastrointestinal (GI) tract (oral exposure). The cytotoxic impact of any substances on the GI tract can be determined by observation of ultrastructure and/or structural cell alterations with the application of

* Corresponding author. Institute of Environmental Sciences, Jagiellonian University, Gronostajowa 7, 30-387, Kraków, Poland.
E-mail addresses: zuza.swiatek@doctoral.uj.edu.pl (Z.M. Świątek), olga.woznicka@uj.edu.pl (O. Woźnicka), bednarska@iop.krakow.pl (A.J. Bednarska).

https://doi.org/10.1016/j.ecoenv.2020.110532
Received 22 December 2019; Received in revised form 19 March 2020; Accepted 21 March 2020

either qualitative (Karpeta-Kaczmarek et al., 2016; Lourenço et al., 2011) or quantitative methods (Amaral and Rodrigues, 2005; Wilczek et al., 2018). Morphometric analysis is a valuable tool for the determination of quantitative changes within tissues/cells and provides data suitable for statistical analysis. This method has been successfully applied to study the toxic effects of nanomaterials in invertebrates (Calisi et al., 2016; Savić-Zdravković et al., 2018). We hypothesize that in the case of earthworms, both epithelial cells and chloragogen cells (chloragocytes) within the GI tract may be directly impacted by NPs and/or ions, affecting the physiology of the organism.

Different theories have been proposed to explain how the toxicity and mechanism of action of ZnO-NPs compares with those of ions at the cellular level. Reactive oxygen species (ROS) generation has been proposed as the main factor of ZnO-NPs toxicity (Fröhlich and Fröhlich, 2016; Unfried et al., 2007). Excessive ROS production is linked with oxidative damage, which can lead to mitochondrial dysfunction and ATP depletion, inhibition of organism respiration and subsequent cell death (Berg et al., 2002; Yu et al., 2013). Clearly, Zn ions, derived from ZnO-NPs dissolution or metal salts, can also induce ATP depletion, e.g., through inhibition of key enzymes in the glycolytic pathway or by direct contribution to mitochondrial cytochrome *c* release, resulting in cell death (Xia et al., 2008). Thus, measurements of ATP levels or its levels relative to those of other adenine nucleotides (e.g., ADP) can be an adequate biomarker for comparison of toxicity between metal ions and NPs (Babczynska et al., 2011; Dziewięcka et al., 2018).

The aim of this study is to understand the nano-specific cytotoxicity of ZnO-NPs versus that of Zn ions in the earthworm *Eisenia andrei*. The research goal is to unravel the mechanistic pathways focusing on 1) if and how gut epithelium and chloragogen cells of the GI tract are altered, 2) to what magnitude changes within chloragogen tissues are seen using morphometric analysis after 48 h of exposure, and 3) if the ADP/ATP ratio at the level of the whole organism is changed after a 21-day exposure and a 14-day recovery period. To address these research questions, a similar experimental set up was used as in earlier studies (Świątek and Bednarska, 2019; Świątek et al., 2017) in which earthworms were exposed to ZnO-NPs or Zn ions in Lufa 2.2 soil. The GI tract was selected as the first barrier for ingested substances, and hence, exposure might be expressed through structural alterations in the gut epithelium and chloragogen cells. Considering that investigating the narrow range of targeted cells under short-term (acute) exposure may give an imprecise estimation of toxicity, the obtained results for the GI tract were compared with the state of the cells at the level of the whole organism using the ADP/ATP ratio measured a few times during long-term (chronic) exposure.

2. Materials and methods

2.1. Soil spiking procedure

Standardized Lufa 2.2 loamy sand soil (Lufa-Speyer 2.2, Germany, 2017) was used (see Supplementary Materials for details). The effects of two concentrations of ZnO-NPs (nominal: 500 and 1000 mg Zn kg^{-1} dry soil, designated ZnO-NPs 500 and ZnO-NPs 1000, respectively), two concentrations of $ZnCl_2$ (nominal: 250 and 500 mg Zn kg^{-1} dry soil, designated $ZnCl_2$ 250 and $ZnCl_2$ 500, respectively), and one control with ca. 27 mg Zn kg^{-1} dry soil (natural Zn level in soil) were studied. The chosen concentrations corresponded to the EC_{25} and EC_{50} for earthworm reproduction (Heggelund et al., 2014) and represented low and medium values of typical total Zn contamination in urban areas (Stafilov et al., 2010; Stefanowicz et al., 2008) and very high concentrations of predicted concentrations for ZnO-NPs (Sun et al., 2014). $ZnCl_2$ (used to represent treatments with ionic Zn) was added as aqueous solutions, and ZnO-NPs were added as a dry powder to the Lufa 2.2 soil. Contaminated soil was mixed with a kitchen robot to obtain homogeneously spiked soil as practically as possible. After dosing the soil, demineralized water was added to all treatments to reach a 50% water holding capacity (WHC) in the soil. Soils were incubated for 7 days at 20 °C before being used in the experiment. The methodology and results of NP characterization are given in the Supplementary Materials.

2.2. Soil physiochemical properties

To analyse the Zn concentration in soil at day 0 (start of the experiment), three samples of soil per treatment were dried at 105 °C for 24 h and weighed to the nearest 0.0001 g. Soil samples were digested in 10 mL of a 4:1 mixture of HNO_3:H_2O_2 using microwave digestion (using the system of Titan MPSTM, PerkinElmer) and then supplemented with 30 mL of demineralized water. Zn concentrations in the solutions were measured using flame atomic absorption spectrometry (AAS) (PerkinElmer AAnalyst 200) and expressed in mg kg^{-1} dry weight (dw). To determine analytical precision, three blanks and three samples of a certified reference material (Sand 1, Sigma-Aldrich, with a certified Zn concentration of 425 ± 9.1 mg kg^{-1}) were examined with the samples. The measured Zn concentrations in the reference material were within 2% of the certified concentrations.

The Zn concentrations in water extracts from soil samples and extracts after ultrafiltration were additionally characterized on days 0, 7, 14 and 21 of the experiment following the method described in Świątek and Bednarska (2019). The soil pH was measured potentiometrically with 0.01 M $CaCl_2$ (1:5 w/v) at days 0, 7, 14 and 21. Soil samples were shaken at room temperature for 2 h at 2000 rpm, and after allowing the floating particles to settle overnight, the pH was measured using a pH meter. The soil organic matter content was determined at days 0 and 21 as loss on ignition.

2.3. Experimental design

The experiment was designed following the procedure described by Świątek and Bednarska (2019). In brief, the toxicokinetic experiment was performed with *E. andrei* earthworms (N = 300) exposed for 21 days to Zn-contaminated soil (contamination phase) and then allowed 14 days of elimination in a non-spiked control soil (decontamination phase). Horse dung (ca. 7 mg dry weight per 1 g dry weight of soil) was added as a source of food at the beginning of each phase prior to introducing the soil into the test containers. Food was added to ensure earthworm growth and well-being, as we expected that in an experiment lasting 35 days, food deprivation might act as an additional stressor (Spurgeon et al., 2003). Before starting the experiment, the earthworms were acclimated to Lufa 2.2 soil for 24 h, and then they were placed in empty Petri dishes lined with moistened filter paper for 24 h to void their gut content, washed in tap water and weighed to the nearest 0.0001 g. Then, worms were randomly assigned to treatments at one individual per container filled with approximately 60 g of wet soil. Containers were kept at 20 °C and 75% relative humidity under a 16:8 h light:dark cycle. Once a week, the moisture of the soil was checked and replenished with tap water when necessary. The details of the *E. andrei* earthworm culture conditions are presented in the Supplementary Materials.

2.4. Gut response measurements

For measurements of structural alterations in the gut epithelium and chloragogen cells of the GI tract using transmission electron microscopy (TEM), five individuals were sampled from each treatment and the control after 48 h of exposure. The period of 48 h was selected based on a previous study showing that the highest concentrations of Zn were accumulated by earthworms on the 2nd day of exposure (Świątek and Bednarska, 2019; Świątek et al., 2017). The details of the midgut dissection and TEM analysis sample preparation are presented in the Supplementary Materials.

For qualitative data recording, 7 and 10 pictures were taken on

average from each treatment for epithelium and chloragogen tissue, respectively. The structural alterations in the gut epithelium (epithelial damage, i.e., dilated intercellular junctions, epithelial flattening, and filling of goblet cells) and chloragogen tissue (shape changes of the cells and presence of the spherites) were recorded and compared to control samples (earthworms from uncontaminated soil).

For morphometric analysis, cell images were randomly captured at 3000–8000 *x* magnification. For each individual, 2–6 chloragogen cells were captured from two sections of the middle gut. This resulted in 12 cells for the control, 24 cells for $ZnCl_2$ 250, 20 cells for $ZnCl_2$ 500, 22 cells for ZnO-NPs 500 and 21 cells for ZnO-NPs 1000. For each chloragogen cell, its area (a_{cell}), the area of the chloragosome granules (a_{CH}), and the area of the debris vesicles (a_D) were measured. Both a_{CH} and a_D were divided by a_{cell} to correct for the possible effect of the size of the chloragogen cell. Thereafter, for each earthworm, average A_{CH}/A_{cell} and A_D/A_{cell} ratios were calculated, and those ratios (A_{CH}/A_{cell}; A_D/A_{cell}) were used for further statistical analysis. The areas of all objects (i.e., a_{cell}, a_{CH}, and a_D) were determined manually using the ImageJ software package. Chloragosome granules and debris vesicles were chosen for measurements because they are easily distinguishable cytoplasmic organelles involved in ionic regulation and metal sequestration (Morgan et al., 2002). The earthworms for which neither chloragosomes nor debris vesicles were observed in any of the studied cells were excluded from further analysis. The methodology scheme applied for quantitative data recording is presented in the Supplementary Materials (Fig. S2).

2.5. ADP/ATP ratio measurements

For ADP/ATP measurements, five individuals were sampled before the exposure was started (day 0) and 1, 2, 4, 7, 14, and 21 days (contamination phase) and 22, 23, 28 and 35 days (decontamination phase) later for each Zn treatment and control. At each sampling point, the collected earthworms were rinsed with tap water, blotted dry on filter paper, and kept individually for 24 h in Petri dishes lined with moistened filter paper to void their gut content. Thereafter, the worms were rinsed, blotted dry, weighed to the nearest 0.0001 g, frozen in liquid nitrogen and stored at −80 °C until further analysis.

Frozen earthworms (whole specimens) were homogenized on ice using a mechanical Omni tissue homogenizer (TH220-PCR). To remove proteins from samples, 2% perchloric acid (Sigma-Aldrich, p. a.) in a 1:4 w/v ratio was added, and vortexed samples were placed on ice for 10 min. Next, samples were centrifuged (5 min, 14 000 *g*, 4 °C), and the supernatants were neutralized with a mixture of 3 M KOH (Avantor Performance, p. a.), 0.4 M Tris (Sigma-Aldrich, p. a.), and 3 M KCl (Avantor Performance, p. a.) to reach pH 7.75–8.0, which is optimal for luciferase activity (Babczynska et al., 2011; Napolitano and Shain, 2005) and vortexed again. After final centrifugation (5 min, 8000 *g*, 4 °C), the samples were immediately used for ADP/ATP ratio luminometric measurements using a Bioluminescence Assay Kit, ApoSENSOR (BioVision Inc.), according to the manufacturer's protocol. Measurements were performed on 96-well plates (OptiPlate-96, PerkinElmer) using an Infinite 200 PRO plate reader (TECAN).

Following the formula provided by the manufacturer, the cellular energetic state of each earthworm was calculated and expressed as the ADP/ATP ratio. According to the manufacturer's manual, the results for ADP/ATP should distinguish four cell states: proliferation, growth arrest, apoptosis and necrosis. The manufacturer did not specify ADP/ATP values for the cell states: instead, a qualitative description is given (see the Supplementary Materials for a detailed description of each state). Therefore, due to the lack of method standardization, based on our own results for ADP/ATP ratios and earthworm body mass and survival, we arbitrarily used the maximum ADP/ATP ratio derived for earthworms sampled at day 0 (before the exposure) as a threshold to distinguish between cell proliferation and all other physiological states of cells (growth arrest, apoptosis and necrosis).

2.6. Data handling and statistical analysis

The distributions of all the studied parameters were checked for normality with Shapiro–Wilk's W test, and the homogeneity of variances was checked with Levene's test. If the criteria were not met, values of the modified z-MAD scores greater than 3.5 in absolute value were treated as outliers and excluded from analysis. Next, the data were either log or square root transformed, and if these steps failed, a non-parametric test was used.

The effect of treatment (on each day) or time (within each treatment) on Zn concentration in water extracts and the pH was tested using the Kruskal-Wallis test, and if significant differences were observed, a Bonferroni procedure was used to identify the pattern of differences between treatments or among days at the 95.0% confidence level.

To verify that individuals assigned to different treatments did not differ in the initial (day 0) body mass, one-way ANOVA was performed. To check whether earthworms lost body mass during the experiment, the body mass change (BMC) index was calculated for each individual based on the mass of the depurated earthworms according to the following equation: $BMC = (M_n - M_0)/M_0$, where M_n is the mass of an earthworm at sampling day *n* (g), and M_0 is the initial mass (at day 0) of the same earthworm (g). The effect of treatment or time on the BMC index was tested with the Kruskal-Wallis test for each phase (contamination and decontamination) separately, and when significant differences were found, a Bonferroni procedure was used to identify the pattern of differences among treatments or sampling days at the 95% confidence level. Moreover, to verify whether the BMC index changed from pre-exposure (day 0) to after exposure (day 21) and recovery (day 35), the Kruskal-Wallis test was separately performed for each treatment with time (limited to days 0, 21 and 35) as a factor.

The effect of treatment on A_D/A_{cell} and A_{CH}/A_{cell} was tested using one-way ANOVA. If significant differences were observed, a post hoc least squares difference (LSD) test was used to identify the pattern of differences among treatments. The effect of treatment and sampling day on the ADP/ATP ratio was separately tested for each phase using two-way ANOVA with body mass (M_n) as a covariate. Day 0, which was common for all treatments, was excluded from the ANOVA to allow for testing interactions between factors. Nonsignificant ($p \geq 0.05$) interaction and/or covariate were removed from the model. If significant differences were observed, a post hoc LSD test was used to identify the pattern of differences among treatments and/or exposure days. To verify whether ADP/ATP ratios after decontamination (day 35) differed from those after the exposure (day 21) and returned to the pre-exposure state (day 0), the Kruskal-Wallis test was performed for each treatment separately with time (limited to days 0, 21 and 35) as a factor.

In all Kruskal-Wallis tests, the Bonferroni correction for multiple comparisons was applied. The data were analysed statistically using Statgraphic Centurion XVI (StatPoint Technologies, Inc., version 18).

3. Results

3.1. Soil physicochemical properties

Zinc concentrations (mean ± SD) measured in the test soil were in accordance with nominal concentrations, and 19.5 ± 0.3 mg Zn kg^{-1} dw was found in the control soil (Table S1). In general, zinc concentrations in the water extracts were lowest for the control, higher than that for both EC_{25} treatments, and highest for both EC_{50} treatments. The zinc concentrations in the water extracts were significantly lower on day 21 than on day 14 in the control treatment ($p = 0.007$). In the $ZnCl_2$ 250 treatment, Zn concentrations were significantly higher at days 0 and 7 than at day 21 ($p = 0.006$), while in the $ZnCl_2$ 500 treatment, Zn concentrations were higher at day 0 than at day 21 ($p = 0.005$). No differences between days were observed in the ZnO-NPs 500 and ZnO-NPs 1000 treatments (Table S1). In the control, $ZnCl_2$

250 and $ZnCl_2$ 500 treatments, the average Zn concentrations in the ultrafiltrates corresponded to 30–70%, 79–90% and 90–94% of the Zn in the water extracts, respectively. In the ZnO-NPs 500 and ZnO-NPs 1000 treatments, the Zn concentrations in the ultrafiltrates corresponded to 36–60% and 54–68% of the Zn in the water extracts (Fig. S3).

The pH measured in soil differed between treatments and days and was higher in soils spiked with ZnO-NPs than in the soils spiked with $ZnCl_2$. Significantly lower pH values were observed at day 7 than at days 0 and 21 in the control ($p = 0.007$). An increase in pH was observed over time, with higher values at day 21 than at day 0 in the $ZnCl_2$ 500 ($p = 0.01$) and ZnO-NPs 500 ($p = 0.004$) treatments and at day 14 than at day 7 in the ZnO-NPs 1000 treatment ($p = 0.002$) (Fig. S4). The average soil organic matter content was similar for all treatments at day 0 (3.5 ± 0.2%) and day 21 (4.6 ± 0.3%).

3.2. Earthworm responses

All the earthworms survived until the end of the experiment. The average initial body mass (± SD) of the earthworms was 0.31 ± 0.07 g (N = 260), with no significant differences between treatments ($p = 0.65$). There was no effect of sampling day on the BMC index in either the contamination ($p = 0.05$) or decontamination ($p = 0.7$) phase (Fig. S5). Treatment had no effect on the BMC index for either of the two phases ($p = 0.8$). There were no differences in the BMC index ($p > 0.03$) among days 0, 21 and 35 for any treatments except $ZnCl_2$ 250, in which earthworms weighed more at day 35 than at day 0 ($p = 0.002$). Although there were no significant differences in the BMC index between days and among the treatments in either the contamination or decontamination phases, there was a large variance in the BMC index in the decontamination phase, suggesting that regardless of treatment, some earthworms grew unevenly in this phase.

3.3. Midgut epithelium

The midgut epithelium of earthworms consists of two types of cells: ciliated and gland (goblet) cells. The ciliated cells are narrow and elongated, and a few of them form a sheath for gland cells. Regionalization of the cytoplasm is observed with the presence of mitochondria in the apical region, the nucleus in the cell centre, the Golgi apparatus in the perinuclear region and the endoplasmic reticulum at the base. The cytoplasm of gland cells is usually filled with vacuoles varying in dimension and number (Kamat, 1956). In the present study, the features that noticeably distinguished control epithelial cells from Zn-treated epithelial cells were a loss of integrity between cells, epithelial flattening, and filling of goblet cells. In comparison with the junctions in the control (Fig. 1A), dilated intercellular junctions were observed in all Zn treatments (Fig. 1B–E), with a relatively higher occurrence of this phenomenon in the ZnO-NPs 1000 treatment than in the other Zn treatments (Fig. 1E). Similarly, epithelial flattening, visible as a corrugation of cell walls, was observed for all Zn treatments, with a slight flattening of the epithelium in ionic treatments (Fig. 1G and H) and a more visible flattening in NP treatments (Fig. 1I and J) in comparison with the control (Fig. 1F). The gland cells of worms from $ZnCl_2$ 500 and ZnO-NPs 500 treatments were visibly larger than the corresponding cells from the control, and this was related to an enlargement of the intracellular vesicles (Fig. 1M and N). We did not find clearly separated gland cells in the $ZnCl_2$ 250 treatment, and this might be a result of their low activity (Fig. 1L). Likewise, gland cells from the ZnO-NPs 1000 treatment were impossible to identify, although in this case, it was due to substantial destruction of the epithelium (Fig. 1O).

3.4. Chloragogen tissue

The chloragogen tissue of earthworms is a diffuse layer of large, usually club-shaped cells (chloragocytes) that separate the blood from the coelomic fluid. The chloragocytes contain an abundance of spherical granules (chloragosomes), debris vesicles and glycogen (Prento, 1979). In metal-stressed worms, incrustations in the form of spherites can be observed (Hopkin, 1989). In the present study, four cell shapes were observed: 1) normal, club-shaped cells, 2) amoeboid-shaped cells, 3) swollen cells, with high numbers of vesicles in the cytoplasm, and 4) necrotic cells. In the majority of the cells from both EC_{25} treatments ($ZnCl_2$ 250 and ZnO-NPs 500) (Fig. 2C and G), no serve alterations in the shape of the chloragocytes were observed in comparison with the control shapes (Fig. 2A). In general, normal physiological variance among cells was observed in EC_{25} treatments and the control, which was manifested by the presence of club-shaped cells and, to some extent, detached amoeboid cells. In the case of EC_{50} treatments ($ZnCl_2$ 500 and ZnO-NPs 1000), amoeboid-like cells were predominantly observed (Fig. 2E and I). In all Zn treatments, dead or swollen cells, with characteristic vesiculation of cytoplasm, were found subjectively in a smaller number in EC_{25} treatments (Fig. 2D and H) than in EC_{50} treatments (Fig. 2F and J). Completely destroyed (necrotic) cells (Fig. 2H) and/or vesiculation of cytoplasm were distinctive for all Zn treatments (Fig. 2D, F, H and J) and not observed in the control treatment. Instead, in the control treatment, a small abundance of worn-out mature cells was observed that were characterized by an amoeboid shape, an increased occurrence of the Golgi apparatus and rough endoplasmic reticulum (Fig. 2B). Regarding cell content, numerous spherites were found in only ionic and not in NP treatments or control (Fig. S6).

3.5. Morphometric analyses

The average earthworm chloragosome granule (A_{CH}) to cell area (A_{cell}) ratio was significantly lower in both EC_{50} treatments than in the control. Significantly higher A_{CH}/A_{cell} ratios were observed for $ZnCl_2$ 250 than for $ZnCl_2$ 500 treatment and for ZnO-NPs 500 treatment than for ZnO-NPs 1000 treatment ($p = 0.001$). Differences in A_{CH}/A_{cell} ratios were also observed for nominal concentrations of 500 mg kg^{-1}, with significantly higher values observed for ZnO-NP treatment than for $ZnCl_2$ treatment ($p = 0.001$, Fig. 3A). The A_D/A_{cell} ratio was significantly higher in the $ZnCl_2$ 500 treatment than in the other treatments and significantly higher in the $ZnCl_2$ 250 treatment than in the ZnO-NPs 500 treatment ($p = 0.002$, Fig. 3B).

3.6. ADP/ATP ratio

In the contamination phase, the ADP/ATP ratio did not differ significantly among treatments ($p = 0.1$), and a close to significant effect of sampling day was observed ($p = 0.08$), with the highest average values of the ADP/ATP ratio found at day 14 at ca. 17% higher than those at day 1 (Fig. 4A and B). In the decontamination phase, neither treatment ($p = 0.1$) nor sampling day ($p = 0.4$) significantly affected the ADP/ATP ratio (Fig. 4A and C). Comparisons of ADP/ATP ratio values between days 0, 21 and 35 for each treatment revealed significantly higher values at day 21 than at day 0 ($p = 0.01$) for the control. In $ZnCl_2$ 250, $ZnCl_2$ 500, and ZnO-NPs 500 treatments, the ADP/ATP ratio was significantly higher at day 35 than at day 0 ($p \leq 0.01$). In the ZnO-NPs 1000 treatment, the ADP/ATP ratio was significantly higher at days 21 and 35 than at day 0 ($p = 0.001$) (Fig. S7). The ADP/ATP ratio for all earthworms, i.e., regardless of treatment, ranged from 1.2 to 3.8 with 50% of values above 2.3 (the threshold above which growth arrest starts) for $ZnCl_2$ 500, 60% of values above 2.3 for the control and ZnO-NPs 500, and 70% for $ZnCl_2$ 250 and ZnO-NPs 1000 in the contamination phase. In the decontamination phase, the ADP/ATP ratio ranged from 1.6 to 3.8 with 40% values above 2.3 for the control, 70% for $ZnCl_2$ 250, 80% for $ZnCl_2$ 500 and ZnO-NPs 500, and 95% for ZnO-NPs 1000.

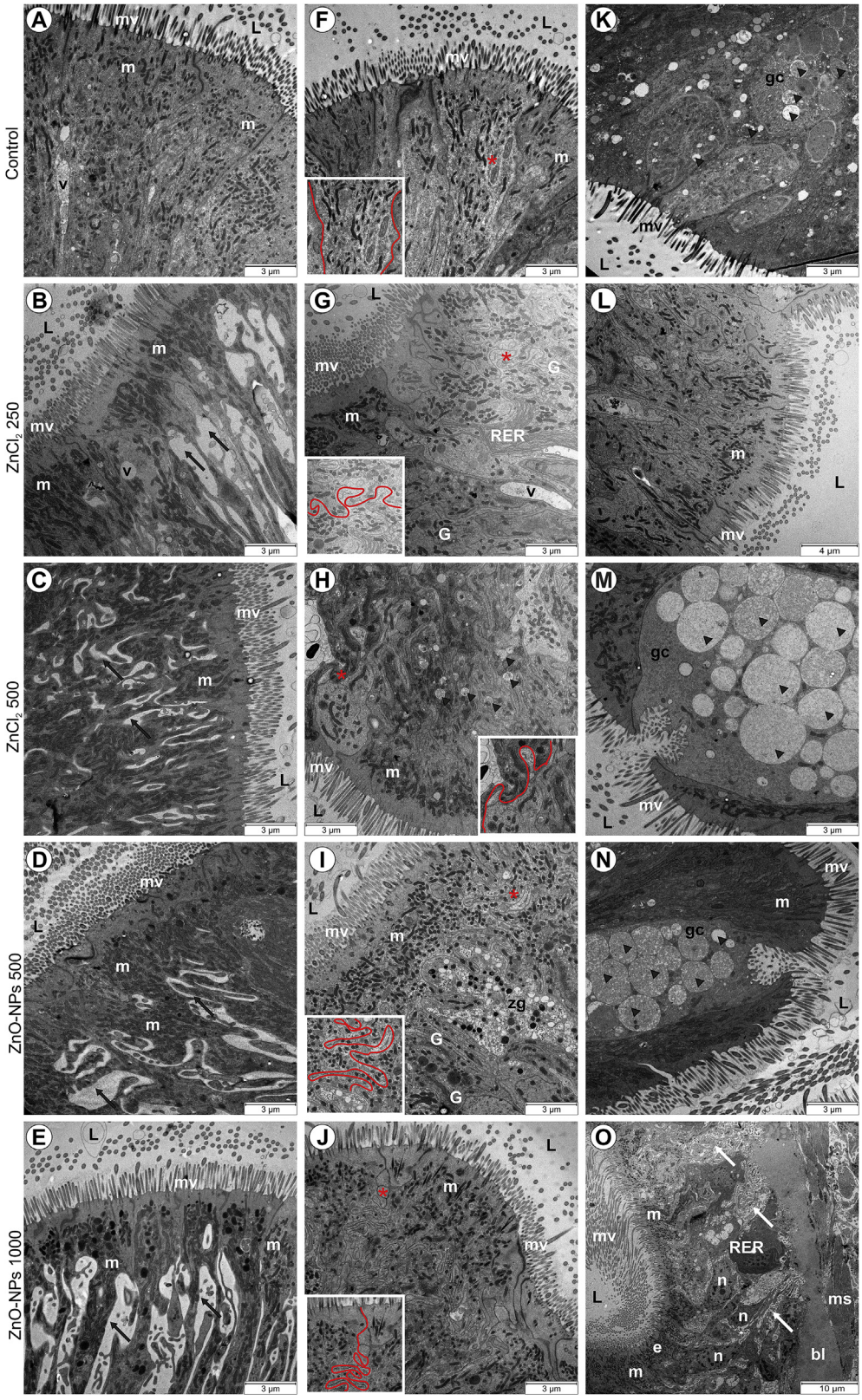

Fig. 1. Electron micrographs of the intestinal epithelium in *Eisenia andrei* earthworms exposed to Lufa 2.2 soil contaminated with different concentrations of Zn nanoparticles (ZnO-NPs) and ions ($ZnCl_2$). Epithelial damage with dilated intercellular junctions, epithelial flattening, and filling of goblet cells is shown in the left, middle, and right columns, respectively. Note that the dilation of junctions is marked with an arrow; epithelial flattening is marked on a small picture in the middle column with a red curve, and a selected place is marked with an asterisk; enlargement of vesicles in goblet cells is marked with an arrow head. Lumen (l), mitochondria (m), microvilli (mv), vacuoles (v), zymogen granules (zg), Golgi apparatus (G), rough endoplasmic reticulum (RER), goblet cell (gc), intestinal epithelium (e), nucleus (n), basal lamina (bl), muscles (ms). (For interpretation of the references to colour in this figure legend, the reader is referred to the Web version of this article.)

4. Discussion

This study shows the mechanistic pathway responsible for differences in the nano-specific toxicity of ZnO-NPs and Zn ions in the earthworm *E. andrei*. We demonstrated a cytotoxic effect of Zn in the form of NPs and ions in the epithelium and chloragogen tissue of *E. andrei* earthworms after their short-term exposure to contaminated soil. A qualitative study revealed the presence of spherites in only the ionic treatments, while morphometric measurements showed that the proportions of debris vesicles in the chloragocytes were lower in worms exposed to NPs than in those exposed to ions, suggesting different manners of regulating Zn forms. The ADP/ATP measurements did not

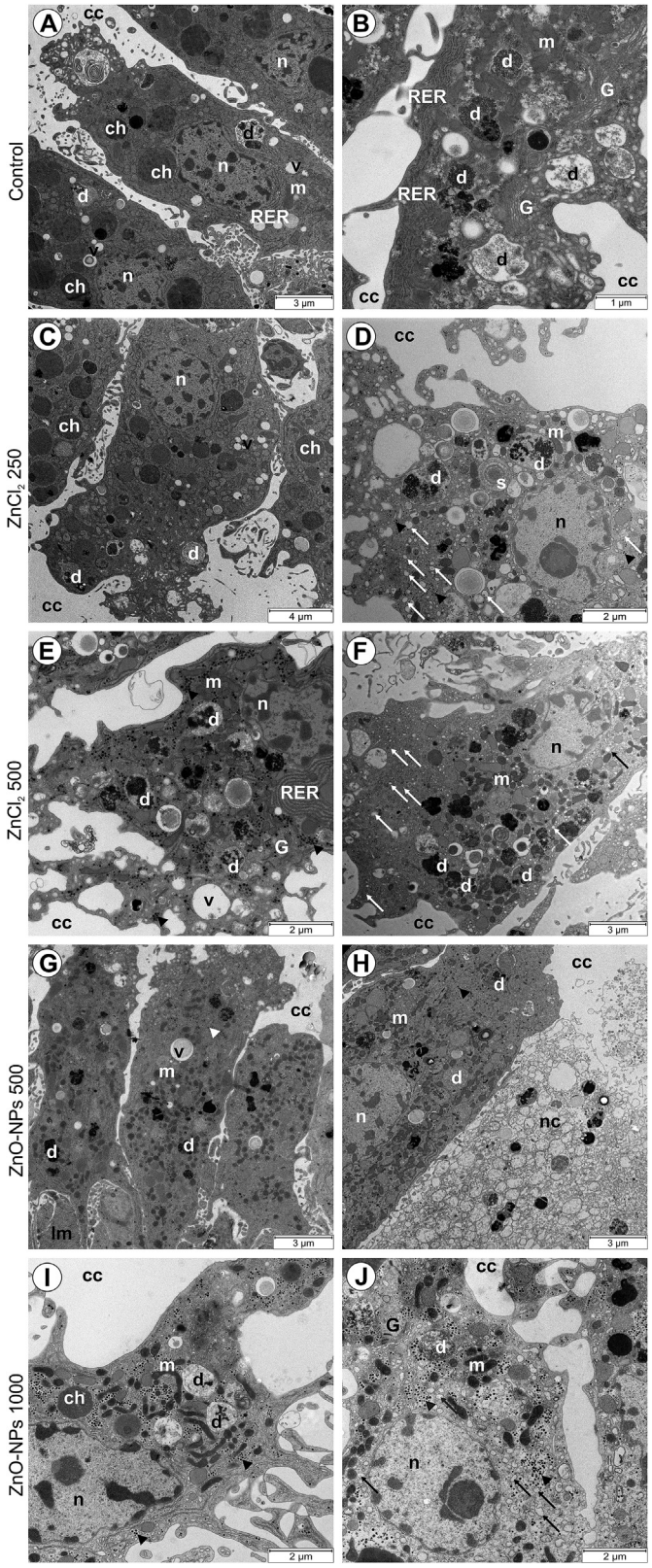

Fig. 2. Electron micrographs of the chloragogen cells (chloragocytes) in *Eisenia andrei* earthworms exposed to Lufa 2.2 soil contaminated with different concentrations of Zn nanoparticles (ZnO-NPs) or ions ($ZnCl_2$). Cell shapes that were found in the vast majority of each treatment are presented in the left column. Cell swelling and vesiculation of the cytoplasm (marked with arrows) are presented in the right column. Coelomic cavity (cc), chloragosome granule (ch), debris vesicle (d), mitochondria (m), vacuoles (v), Golgi apparatus (G), rough endoplasmic reticulum (RER), nucleus (n), spherite granule (s), necrotic cell (nc).

indicate the cytotoxic effect of Zn at the whole-body level, with no differences between Zn treatments and control in either the contamination or decontamination phases. However, compared with pre-exposure ratios (day 0), increased ADP/ATP ratios were observed for all Zn treatments except the control at the end of decontamination phase (day 35). This suggests that even after the completion of Zn long-term exposure, cellular damage may accumulate, leading to adverse effects on the physiology of the organism at the whole-body level.

4.1. Zn partitioning in soil

Differences in Zn partitioning and soil pH were observed for the examined forms of Zn with results consistent with those of previous studies (Romero-Freire et al., 2017; Świątek et al., 2017). In both ionic treatments, a significant decrease in the Zn concentration in the water extract was observed, which might be related to metal adsorption to organic matter and clay minerals in the solid phase or complexation with ligands that are large enough to not enter the solution phase of the extract (Degryse et al., 2009). The lack of changes in the water extract Zn concentrations in ZnO-NPs 500 and ZnO-NPs 1000 treatments might be associated with simultaneous, opposing physicochemical transformations of NPs, such as dissolution and aggregation (Goswami et al., 2017). Differences between ionic and NP treatments were also observed for pH, which was clearly lower in $ZnCl_2$ treatments than in NP treatments. This phenomenon may be associated with the metal salt having higher solubility than NPs; as zinc chloride releases Zn^{2+}, which is prone to competition with other cations. Soil acidification in metal salt-amended soils was also observed by García-Gómez et al. (2015) and Speir et al. (1999).

4.2. Earthworm responses

4.2.1. Qualitative structural changes in the epithelium and chloragogen tissue

TEM imaging showed pronounced changes in the ultrastructure of the gut epithelium in the Zn treatments in comparison with that of control earthworms. A marked intensity of this phenomenon was observed for the treatment with the highest Zn concentration, i.e., ZnO-NPs 1000. Dilation of the spaces at the basal plasma membrane level and reduction in thickness of the gut epithelium were observed for all Zn treatments, with some differences in the intensity of epithelial flattening between NP and ionic treatments. Enlargement of the intracellular vesicles in gland cells was mainly observed for $ZnCl_2$ 500 and ZnO-NPs 500 treatments. Similar to our study, Kaya et al. (2016) observed hypertrophic gland cells in the epithelium of tilapia (*Oreochromis niloticus*) after they were exposed to small and large (10–30 nm and 100 nm, respectively) ZnO-NPs at concentrations of 1 and 10 mg L^{-1}. The authors indicated that gland cell hypertrophy, in which cells increase in volume due to an enlargement of their components, might be associated with excessive mucus production. Other authors discussed that mucus, both excreted outside the body and remaining inside the digestive tracts, probably acts as a defence system when earthworms are exposed to unpleasant or even harmful conditions (Morgan et al., 1999). Therefore, in the present study, gland cell hypertrophy was most likely associated with a volumetric increase in vacuoles responsible for mucus production, which can be considered an adaptive response activated to defend the cell against excessive amounts of Zn.

Reduction in the epithelial width was predominantly detected in earthworms exposed to the ZnO nanoform, and to a lesser extent, reduction was induced by Zn ions. Such qualitative data do not entitle us, however, to state that NPs caused a significantly greater effect. Changes in epithelial thickness have been observed in invertebrates exposed to both metal ions and NPs (Amaral and Rodrigues, 2005; Bacchetta et al., 2014; Lourenço et al., 2011). The dilation of intracellular spaces (i.e., the changes observed in this study) together with epithelium atrophy

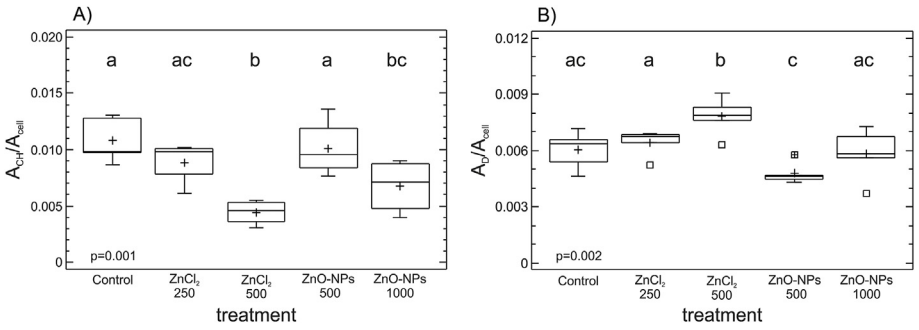

Fig. 3. Average chloragosome granule to cell area ratio, A_{CH}/A_{cell} (A), and debris vesicles to cell area ratio, A_D/A_{cell} (B), in chloragogen tissue of *Eisenia andrei* earthworms exposed to Lufa 2.2 soil contaminated with different concentrations of Zn nanoparticles (ZnO-NPs) or ions ($ZnCl_2$). Boxes – lower and upper quartiles, whiskers – extend to the minimum and maximum values, plus sign – mean value, centre line – median, empty squares (outliers) – between > 1.5 and 3 times the interquartile range, squares with plus sign (far outliers) – more than 3 times the interquartile range. Different letters represent significant differences between treatments (ANOVA, LSD, $p < 0.05$).

were considered initial processes of gut necrosis in *E. andrei* earthworms when exposed to soil contaminated with metals and radionuclides (Lourenço et al., 2011) and *L. terrestris* earthworms collected from metal-contaminated volcanic soils (Amaral and Rodrigues, 2005).

While gland cell hypertrophy might be considered an adaptive response, both epithelial flattening and the dilation of cellular spaces are harmful and deleterious, possibly leading to digestion failure (Rocha et al., 2016), impaired nutrient absorption, and, as a consequence, weight loss. In our study, no weight loss was noted, but there was also no weight gain, which may have been partly the result of an impaired digestive system. Our data indicate that ultrastructure changes in the gut epithelium seem to be concentration related in *E. andrei*. Nevertheless, differences between treatments that were determined from qualitative structural changes in the epithelium seem to be not reflected in the metabolic state of the cells as determined by the ADP/ATP ratio, as no differences between treatments, and therefore between Zn forms, were found for ADP/ATP.

Earthworm chloragogen tissue has received extensive attention in metal toxicity studies (Andre et al., 2009; Cancio et al., 1995; Morgan et al., 2002). Chloragogen tissue has been recognized as having many functions, such as balancing cation and pH levels in the blood and coelomic fluid; the synthesis of haemoglobin; and, most importantly, the accumulation and detoxification of metals (Cancio et al., 1995; Morgan et al., 2002). Similar to the changes observed in the epithelium, a qualitative study of the chloragocytes revealed that chloragocytes were visibly different in Zn-treated earthworms than in control earthworms, and the most pronounced difference was manifested in vesiculation of the cytoplasm. Broad vesiculation of chloragocyte cytoplasm was likewise observed in *E. fetida* earthworms exposed for 3–5 weeks to sublethal concentrations of lead (500 mg kg^{-1}) in soil (Cancio et al., 1995). Cell swelling, bubble formation and blister formation are typical characteristic of necrosis (D'Herde et al., 2009); therefore, it is probable that this type of cell death has also occurred to some extent in all Zn-treated earthworms in the present study. Although deformation and vesiculation of chloragocytes, followed by cell death, might result in impaired metabolic and homeostatic functions in chloragogen tissue, the changes observed after acute exposure (48 h) were not reflected in the earthworm metabolism after chronic exposure (21 days) and recovery (14 days). Importantly, no differences were observed for those alterations between the NP and ionic treatments.

One of the most interesting findings in our study, related to cell content, concerns the presence of spherites in the ionic treatments but not the NP treatments. Spherites, recognized as concentrically structured type A granules, are associated with the intracellular precipitation of calcium and magnesium phosphates and the incorporation of increased concentrations of zinc and lead ions (Hopkin, 1989). Thus, their presence may be the result of an adaptive mechanism aimed at protecting against the harmful effects of ionic zinc by binding it in concentric granules. The occurrence of spherites only in worms from the ionic, but not the NP treatments, could be due to: 1) the presence of NPs, to a certain degree, in the pristine (undissolved) form, with only a small share of released ions and/or 2) higher availability of Zn ions in soils with lower pH values. Uneven ion release was reflected in the percentage of total Zn concentration in water extracts recovered after ultrafiltration with ca. 2 times lower ion levels in NP treatments than in ionic treatments at days 0 and 7 (Fig. S2). It seems that in the NP treatments, ionic Zn concentrations were not high enough to promote the production of spherite granules, and thus regulation and immobilization of NPs in earthworm chloragocytes occurred in a different way than they did in the case of ions. Moreover, considering that the lower the pH, the more Zn ions are available to soil dwelling-organisms (Spurgeon and Hopkin, 1996; Waalewijn-Kool et al., 2013), the lower pH values detected in both ionic treatments ($ZnCl_2$ 250 and $ZnCl_2$ 500) could have been responsible for the higher Zn availability and thus for

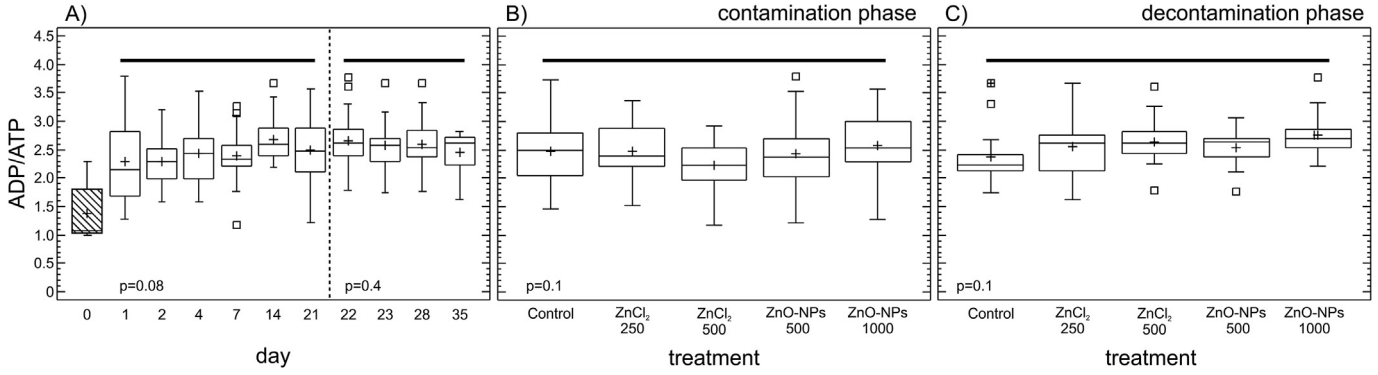

Fig. 4. ADP/ATP ratio in *Eisenia andrei* earthworms exposed to Lufa 2.2 soil contaminated with different concentrations of Zn nanoparticles (ZnO-NPs) or ions ($ZnCl_2$). Boxes – lower and upper quartiles, whiskers – extend to the minimum and maximum values, plus sign – mean value, centre line – median, empty squares (outliers) – between > 1.5 and 3 times the interquartile range, squares with plus sign (far outliers) – more than 3 times the interquartile range. The vertical broken line indicates the start of the decontamination phase. The solid horizontal line indicates no significant differences (ANOVA, LSD, $p < 0.05$) between treatments or between days.

the activation of spherite formation only in those treatments.

4.2.2. Morphometric analyses

In unstressed earthworms, chloragocytes (chloragogen cells) are to a large extent (ca. 40%) filled with a single membrane-bounded organelle called chloragosomes (Prentø, 1987). Under stress, however, increased numbers of debris vesicles, which are the final destinations of cellular organelle remnants and soluble intracellular material, are observed (Andre et al., 2009). Debris vesicles have been proposed as a manifestation of the lifecycle of chloragosomes; they are visible as organelles in a variety of degenerative stages, which can be observed especially when worms are exposed to unfavourable conditions (Andre et al., 2009; Morgan et al., 2002). The morphometric techniques employed in our study demonstrated an effective concentration-related decrease in chloragosome area in relation to cell area. Similar results, with a decreased percentage volume fraction occupied by chloragosomes and inversely correlated with Zn body burdens, were found for the earthworm *Dendrodrilus rubidus* collected from metal-contaminated sites (Morgan et al., 2002). Morgan et al. (2002) suggested the destruction of chloragosomes and their replacement by the formation of debris vesicles as a presumable mechanism of metal immobilization and detoxification.

The differences in the A_D/A_{cell} ratio observed in this study between the ionic and NP treatments were most likely associated with different responses of cell components to different forms of Zn and their bioavailability: for increased ionic Zn concentrations, the ratio increased by 7% and 30% in the $ZnCl_2$ 250 and 500 treatments, respectively, while the ratio decreased by 21% and 3% in the ZnO-NPs 500 and 1000 treatments, respectively, compared with the control ratio. Interestingly, the results in this study were to some extent similar to the results of our previous study that had a similar experimental design and treatments, where a significantly lower assimilation rate (k_a) and significantly higher elimination rate (k_e) were observed for the $ZnCl_2$ 500 treatment than for the other treatments when the kinetic parameters were related to the porewater concentrations (Świątek et al., 2017). This was explained by higher availability of Zn in the ionic treatment, which was associated with low pH levels. It is therefore probable that in the present study, increased debris formation in the ionic treatments was due to, in general, lower soil pH levels, followed by increased availability of Zn. Clearly, free available ions must have also been released from the soil in the ZnO-NPs 1000 treatment as there were no differences in the A_D/A_{cell} ratio between the $ZnCl_2$ 250 and ZnO-NPs 1000 treatments. Nevertheless, it seems that bioavailable Zn caused higher cellular turnover, i.e., intensified sequestration and detoxification through debris vesicles. One of the enzymes that might take part in the sequestration of ions but not NPs is acid phosphatase, as it is associated with chloragosome activity (Cancio et al., 1995). For instance, Hu et al. (2012) observed, compared with the control activity, significantly higher activity of acid phosphatase after a 14-day exposure of *E. fetida* earthworms to $AgNO_3$ at 500 mg Ag kg^{-1} and significantly lower activity after exposure to the same concentration of Ag-NPs. Determining the exact cellular mechanism behind these differences needs to be further studied.

4.2.3. ADP/ATP ratio

The metabolic state of the cells measured at the level of the whole organism did not differ among treatments and days, in either the contamination or decontamination phase. Nevertheless, a clear trend of the ADP/ATP ratio being elevated compared to its day 0 value was found for all sampling days and treatments, with significant differences between pre-exposure (day 0) and the last day of exposure (day 21) in the treatment with the highest nominal Zn concentration (ZnO-NPs 1000) and the control. Thus, the observed progressive metabolic changes could be due to not only Zn exposure but also other factors, such as the response of earthworms to changes in the soil type, handling (Arnaud et al., 2000) or imbalance in the elemental composition of the studied soil. On the other hand, the fact that the ADP/ATP ratio remained at elevated levels after decontamination was completed (day 0 vs. day 35) in all Zn treatments but not in the control indicates that earthworms were somehow affected by the previous exposure to Zn. Surprisingly, these results contradict results from our previous study, where, e.g., cellular energy reserves (proteins, carbohydrates and lipids) returned to their levels before Zn exposure (Świątek and Bednarska, 2019). The reason is unclear but may be the different sensitivities of different biomarkers.

In the present study, measurements of the ADP/ATP ratio at the whole-body level revealed that the metabolic state of the cells from Zn treatments was only slightly affected by metal exposure, with no differences between ions and NPs. Similar ADP/ATP ratios were above 2.3 (i.e., the threshold distinguishing proliferating and non-proliferating cells) in all studied treatments in the contamination phase (i.e., between 50 and 70%), while in the decontamination phase, only 40% of the values were above 2.3 in the control; however, as many as 70–95% of the values were above that threshold in Zn treatments. This indicates that at least three-quarters of the cells measured in earthworms from Zn treatments were in non-proliferation states in the decontamination phase. Regardless of this high percentage of cells with low viability and/or death, no injuries or mortality were observed at the whole-body level; therefore, the threshold value of 2.3 should be treated in this case as a proxy rather than as a direct indicator of earthworm well-being. Based on structural alterations in the gut epithelium and chloragogen tissue and no significant changes in the BMC index (i.e., no weight gain or loss), it is probable that growth of the cells ceased and that cells died via programmed death or necrosis more frequently in the epithelium and chloragogen tissue of the GI tract than in other parts of the body. Whether the changes observed in the GI tract accumulate under prolonged exposure to either EC_{25} or EC_{50} values for reproduction, leading to a reduction in growth, vitality and fitness, needs to be further studied.

5. Conclusions

Zinc as both ions and NPs caused cytotoxic effects in the earthworm GI tract that were visible as dilated intercellular junctions, tissue flattening, and filling of goblet cells in the epithelium and as cell swelling and vesiculation of cytoplasm in chloragocytes. The application of an unsophisticated morphometric method shed light on significantly different proportions of debris vesicles within the chloragocytes, which depended on the Zn form (ions vs. NPs). Differences were also reflected in the presence of spherites in ionic but not NP treatments. Both debris vesicles and spherite formation were probably associated with free Zn availability. The degenerative changes observed for Zn treatments at the cellular level in the GI tract were not reflected in changes in the ADP/ATP ratio. Interestingly, in the earthworms previously exposed to Zn, the ADP/ATP ratio did not return to its state from before the exposure, indicating a smaller percentage of proliferating cells at the end of the experiment in Zn treatments than in the control. Our study provides new insights into the mechanisms of nano-specific effects that are distinctive from ion regulation inside the GI tract and furthers our understanding of the relationship between the effects observed at the cellular and whole-body levels.

CRediT authorship contribution statement

Zuzanna M. Świątek: Conceptualization, Methodology, Investigation, Formal analysis, Resources, Writing - original draft, Visualization, Funding acquisition. **Olga Woźnicka:** Methodology, Investigation, Writing - review & editing. **Agnieszka J. Bednarska:** Conceptualization, Formal analysis, Writing - review & editing, Supervision.

Acknowledgements

The authors are grateful for assistance in earthworm dissection from A. M. Labecka. We also thank M.G. Vijver for her invaluable comments that helped improve the manuscript.

Appendix A. Supplementary data

Supplementary data to this article can be found online at https://doi.org/10.1016/j.ecoenv.2020.110532.

Funding

This study was financed by the National Science Centre, Poland, project PRELUDIUM (2015/17/N/NZ8/01576) and the Polish Ministry of Science and Higher Education (DS/MND/WBiNoZ/INoŚ/22/2016). Zuzanna Świątek was supported by the National Science Centre, Poland, project ETIUDA (2018/28/T/NZ8/00280).

Declarations of interest

None.

References

Adam, V., Nowack, B., 2017. European country-specific probabilistic assessment of nanomaterial flows towards landfilling, incineration and recycling. Environ. Sci. Nano 4, 1961–1973.

Ajdary, M., Moosavi, M.A., Rahmati, M., Falahati, M., Mahboubi, M., Mandegary, A., Jangjoo, S., Mohammadinejad, R., Varma, R.S., 2018. Health concerns of various nanoparticles: a review of their *in vitro* and *in vivo* toxicity. Nanomaterials 8, 634.

Amaral, A.F., Rodrigues, A.D.S., 2005. Metal accumulation and apoptosis in the alimentary canal of *Lumbricus terrestris* as a metal biomarker. Biometals 18, 199–206.

Amorim, M.J., Roca, C.P., Scott-Fordsmand, J.J., 2015. Effect assessment of engineered nanoparticles in solid media – current insight and the way forward. Environ. Pollut. 218, 1370–1375.

Andre, J., Charnock, J., Sturzenbaum, S.R., Kille, P., Morgan, A.J., Hodson, M.E., 2009. Accumulated metal speciation in earthworm populations with multigenerational exposure to metalliferous soils: cell fractionation and high-energy synchrotron analyses. Environ. Sci. Technol. 43, 6822–6829.

Arnaud, C., Saint-Denis, M., Narbonne, J.F., Soler, P., Ribera, D., 2000. Influences of different standardised test methods on biochemical responses in the earthworm *Eisenia fetida andrei*. Soil Biol. Biochem. 32, 67–73.

Babczynska, A., Wilczek, G., Wilczek, P., Szulinska, E., Witas, I., 2011. Metallothioneins and energy budget indices in cadmium and copper exposed spiders *Agelena labyrinthica* in relation to their developmental stage, gender and origin. Comp. Biochem. Physiol. Toxicol. Pharmacol. 154, 161–171.

Bacchetta, R., Moschini, E., Santo, N., Fascio, U., Del Giacco, L., Freddi, S., Camatini, M., Mantecca, P., 2014. Evidence and uptake routes for zinc oxide nanoparticles through the gastrointestinal barrier in *Xenopus laevis*. Nanotoxicology 8, 728–744.

Berg, J.M., Tymoczko, J.L., Stryer, L., 2002. Biochemistry, fifth ed. Freeman W.H., New York 2002. Section 18.6, The regulation of cellular respiration is governed primarily by the need for ATP. Available from: https://www.ncbi.nlm.nih.gov/books/NBK22448/.

Buerki-Thurnherr, T., Xiao, L., Diener, L., Arslan, O., Hirsch, C., Maeder-Althaus, X., Grieder, K., Wampfler, B., Mathur, S., Wick, P., Krug, H.F., 2013. *In vitro* mechanistic study towards a better understanding of ZnO nanoparticle toxicity. Nanotoxicology 7, 402–416.

Calisi, A., Grimaldi, A., Leomanni, A., Lionetto, M.G., Dondero, F., Schettino, T., 2016. Multibiomarker response in the earthworm *Eisenia fetida* as tool for assessing multi-walled carbon nanotube ecotoxicity. Ecotoxicology 25, 677–687.

Cancio, I., Gwynn, I., Ireland, M.P., Cajaraville, M.P., 1995. The effect of sublethal lead exposure on the ultrastructure and on the distribution of acid phosphatase activity in chloragocytes of earthworms (Annelida, Oligochaeta). Histochem. J. 27, 965–973.

Data, Knowledge on Nanomaterials, 2019. DaNa Database: Information about Nanomaterials and their Safety Assessment. Available from: https://www.nanopartikel.info/en/nanoinfo/knowledge-base#material=material/14, Accessed date: 11 April 2019.

Degryse, F., Smolders, E., Parker, D.R., 2009. Partitioning of metals (Cd, Co, Cu, Ni, Pb, Zn) in soils: concepts, methodologies, prediction and applications – a review. Eur. J. Soil Sci. 60, 590–612.

D'Herde, K., Diez-Fraile, A., Lammens, T., 2009. Apoptotic, autophagic and necrotic cell death types in pathophysiological conditions: morphological and histological aspects. In: Krysko, D.V., Vandenabeele, P. (Eds.), Phagocytosis of dying cells: from molecular mechanisms to human diseases. Springer, Dordrecht, NL, pp. 33–62.

Dziewięcka, M., Witas, P., Karpeta-Kaczmarek, J., Kwaśniewska, J., Flasz, B., Balin, K., Augustyniak, M., 2018. Reduced fecundity and cellular changes in *Acheta domesticus* after multigenerational exposure to graphene oxide nanoparticles in food. Sci. Total Environ. 635, 947–955.

Fröhlich, E., Fröhlich, E., 2016. Cytotoxicity of nanoparticles contained in food on intestinal cells and the gut microbiota. Int. J. Mol. Sci. 17, 509.

García-Gómez, C., Babin, M., Obrador, A., Álvarez, J.M., Fernández, M.D., 2015. Integrating ecotoxicity and chemical approaches to compare the effects of ZnO nanoparticles, ZnO bulk, and $ZnCl_2$ on plants and microorganisms in a natural soil. Environ. Sci. Pollut. Res. 22, 16803–16813.

Goswami, L., Kim, K.H., Deep, A., Das, P., Bhattacharya, S.S., Kumar, S., Adelodun, A.A., 2017. Engineered nano particles: nature, behavior, and effect on the environment. J. Environ. Manag. 196, 297–315.

Heggelund, L.R., Diez-Ortiz, M., Lofts, S., Lahive, E., Jurkschat, K., Wojnarowicz, J., Cedergreen, N., Spurgeon, D., Svendsen, C., 2014. Soil pH effects on the comparative toxicity of dissolved zinc, non-nano and nano ZnO to the earthworm *Eisenia fetida*. Nanotoxicology 8, 559–572.

Hong, T.K., Tripathy, N., Son, H.J., Ha, K.T., Jeong, H.S., Hahn, Y.B., 2013. A comprehensive *in vitro* and *in vivo* study of ZnO nanoparticles toxicity. J. Mater. Chem. B 1, 2985–2992.

Hopkin, S.P., 1989. Ecophysiology of Metals in Terrestrial Invertebrates. Elsevier Applied Science, Barking, UK.

Hu, C., Li, M., Wang, W., Cui, Y., Chen, J., Yang, L., 2012. Ecotoxicity of silver nanoparticles on earthworm *Eisenia fetida*: responses of the antioxidant system, acid phosphatase and ATPase. Toxicol. Environ. Chem. 94, 732–741.

Kamat, D.N., 1956. The structure of the Golgi elements and mitochondria in earthworms and lamellibranchs. Proc. Indian Acad. Sci. B 44, 91–107.

Karpeta-Kaczmarek, J., Augustyniak, M., Rost-Roszkowska, M., 2016. Ultrastructure of the gut epithelium in *Acheta domesticus* after long-term exposure to nanodiamonds supplied with food. Arthropod Struct. Dev. 45, 253–264.

Kaya, H., Aydın, F., Gürkan, M., Yılmaz, S., Ates, M., Demir, V., Arslan, Z., 2016. A comparative toxicity study between small and large size zinc oxide nanoparticles in tilapia (*Oreochromis niloticus*): organ pathologies, osmoregulatory responses and immunological parameters. Chemosphere 144, 571–582.

Kwak, J.I., An, Y.-J., 2015. Ecotoxicological effects of nanomaterials on earthworms: a review. Hum. Ecol. Risk Assess. 21, 1566–1575.

Loureiro, S., Tourinho, P.S., Cornelis, G., Van Den Brink, N.W., Díez-Ortiz, M., Vázquez-Campos, S., Pomar-Portillo, V., Svendsen, C., Van Gestel, C.A.M., 2018. Nanomaterials as soil pollutants. In: Duarte, A.C., Cachada, A., Rocha-Santos, T. (Eds.), Soil Pollution. Academic Press, Cambridge, MA, pp. 161–190.

Lourenço, J., Silva, A., Carvalho, F., Oliveira, J., Malta, M., Mendo, S., Gonçalves, F., Pereira, R., 2011. Histopathological changes in the earthworm *Eisenia andrei* associated with the exposure to metals and radionuclides. Chemosphere 85, 1630–1634.

Morgan, A.J., Stürzenbaum, S.R., Winters, C., Kille, P., 1999. Cellular and molecular aspects of metal sequestration and toxicity in earthworms. Invertebr. Reprod. Dev. 36, 17–24.

Morgan, A.J., Turner, M.P., Morgan, J.E., 2002. Morphological plasticity in metal-sequestering earthworm chloragocytes: morphometric electron microscopy provides a biomarker of exposure in field populations. Environ. Toxicol. Chem. 21, 610–618.

Napolitano, M.J., Shain, D.H., 2005. Quantitating adenylate nucleotides in diverse organisms. J. Biochem. Biophys. Methods 63, 69–77.

Prento, P., 1979. Metals and phosphate in the chloragosomes of *Lumbricus terrestris* and their possible physiological significance. Cell Tissue Res. 196, 123–134.

Prentø, P., 1987. Distribution of 20 enzymes in the midgut region of the earthworm, *Lumbricus terrestris* L., with particular emphasis on the physiological role of the chloragog tissue. Comp. Biochem. Physiol. A Physiol. 87, 135–142.

Rajput, V.D., Minkina, T.M., Behal, A., Sushkova, S.N., Mandzhieva, S., Singh, R., Gorovtsov, A., Tsitsuashvili, V.S., Purvis, W.O., Ghazaryan, K.A., Movsesyan, H.S., 2018. Effects of zinc-oxide nanoparticles on soil, plants, animals and soil organisms: a review. Environ. Nanotechnol. Monit. Manag. 9, 76–84.

Rocha, T.L., Sabóia-Morais, S.M.T., Bebianno, M.J., 2016. Histopathological assessment and inflammatory response in the digestive gland of marine mussel *Mytilus galloprovincialis* exposed to cadmium-based quantum dots. Aquat. Toxicol. 177, 306–315.

Romero-Freire, A., Lofts, S., Martín Peinado, F.J., van Gestel, C.A.M., 2017. Effects of aging and soil properties on zinc oxide nanoparticle availability and its ecotoxicological effects to the earthworm *Eisenia andrei*. Environ. Toxicol. Chem. 36, 137–146.

Savić-Zdravković, D., Jovanović, B., Đurđević, A., Stojković-Piperac, M., Savić, A., Vidmar, J., Milošević, D., 2018. An environmentally relevant concentration of titanium dioxide (TiO_2) nanoparticles induces morphological changes in the mouthparts of *Chironomus tentans*. Chemosphere 211, 489–499.

Speir, T.W., Kettles, H.A., Percival, H.J., Parshotam, A., 1999. Is soil acidification the cause of biochemical responses when soils are amended with heavy metal salts? Soil Biol. Biochem. 31, 1953–1961.

Spurgeon, D., Hopkin, S., 1996. Effects of variations of the organic matter content and pH of soils on the availability and toxicity of zinc to the earthworm *Eisenia fetida*. Pedobiologia 40, 80–96.

Spurgeon, D.J., Weeks, J.M., Van Gestel, C.A.M., 2003. A summary of eleven years progress in earthworm ecotoxicology. Pedobiologia 47, 588–606.

Stafilov, T., Sajn, R., Pancevski, Z., Boev, B., Frontasyeva, M.V., Strelkova, L.P., 2010. Heavy metal contamination of topsoils around a lead and zinc smelter in the republic of Macedonia. J. Hazard Mater. 175, 896–914.

Stefanowicz, A.M., Niklinska, M., Laskowski, R., 2008. Metals affect soil bacterial and fungal functional diversity differently. Environ. Toxicol. Chem. 27, 591–598.

Sun, T.Y., Gottschalk, F., Hungerbuhler, K., Nowack, B., 2014. Comprehensive probabilistic modelling of environmental emissions of engineered nanomaterials. Environ. Pollut. 185, 69–76.

Świątek, Z.M., Bednarska, A.J., 2019. Energy reserves and respiration rate in the earthworm *Eisenia andrei* after exposure to zinc in nanoparticle or ionic form. Environ. Sci.

Pollut. Res. 26, 24933–24945.
Świątek, Z.M., van Gestel, C.A.M., Bednarska, A.J., 2017. Toxicokinetics of zinc-oxide nanoparticles and zinc ions in the earthworm *Eisenia andrei*. Ecotoxicol. Environ. Saf. 143, 151–158.
Unfried, K., Albrecht, C., Klotz, L.-O., Von Mikecz, A., Grether-Beck, S., Schins, R.P.F., 2007. Cellular responses to nanoparticles: target structures and mechanisms. Nanotoxicology 1, 52–71.
Waalewijn-Kool, P.L., Ortiz, M.D., Lofts, S., van Gestel, C.A., 2013. The effect of pH on the toxicity of zinc oxide nanoparticles to *Folsomia candida* in amended field soil. Environ. Toxicol. Chem. 32, 2349–2355.
Wilczek, G., Wiśniewska, K., Kozina, B., Wilczek, P., Rost-Roszkowska, M., Stalmach, M., Skowronek, M., Kaszuba, F., 2018. Effects of food contaminated with cadmium and copper on hemocytes of *Steatoda grossa* (Araneae: Theridiidae). Ecotoxicol. Environ. Saf. 149, 267–274.
Xia, T., Kovochich, M., Liong, M., Mädler, L., Gilbert, B., Shi, H., Yeh, J.I., Zink, J.I., Nel, A.E., 2008. Comparison of the mechanism of toxicity of zinc oxide and cerium oxide nanoparticles based on dissolution and oxidative stress properties. ACS Nano 2, 2121–2134.
Yu, K.N., Yoon, T.J., Minai-Tehrani, A., Kim, J.E., Park, S.J., Jeong, M.S., Ha, S.W., Lee, J.K., Kim, J.S., Cho, M.H., 2013. Zinc oxide nanoparticle induced autophagic cell death and mitochondrial damage via reactive oxygen species generation. Toxicol. Vitro 27, 1187–1195.